Available online at www.sciencedirect.com
ScienceDirect
Journal of Power Sources 163 (2006) 604–615
JOURNAL OF POWER SOURCES
www.elsevier.com/locate/jpowsour

Power quality improvement of a stand-alone power system subjected to various disturbances

Shameem Ahmad Lone *, Mairaj Ud-Din Mufti

Electrical Engineering Department, National Institute of Technology, Srinagar-190006, J&K, India

Received 9 June 2006; received in revised form 8 August 2006; accepted 14 September 2006
Available online 1 November 2006

Abstract

In wind-diesel stand-alone power systems, the disturbances like random nature of wind power, turbulent wind, sudden changes in load demand and the wind park disconnection effect continuously the system voltage and frequency. The satisfactory operation of such a system is not an easy task and the control design has to take in to account all these subtleties. For maintaining the power quality, generally, a short-term energy storage device is used. In this paper, the performance of a wind-diesel system associated with a superconducting magnetic energy storage (SMES) system is studied. The effect of installing SMES at wind park bus/load bus, on the system performance is investigated. To control the exchange of real and reactive powers between the SMES unit and the wind-diesel system, a control strategy based on fuzzy logic is proposed. The dynamic models of the hybrid power system for most common scenarios are developed and the results presented.

Keywords: Wind; Stand-alone power systems; Energy storage

1. Introduction

In most of the countries worldwide, there are remote communities, which are not served by the main electrical grids and may never be connected to them because of economical reasons. Diesel generators are mainly used to serve them. But numerous remote areas have significant wind energy potential. Wind-diesel hybrid power systems are increasingly being seen as a viable and economical alternative to grid supply for such locations. One major advantage of a wind energy based stand-alone power system is that it reduces diesel fuel consumption. However, such stand-alone power systems are characterized by low inertia and poor reactive power support and therefore face wide voltage and frequency variations due to changes in load demand. The integration of wind turbines in such systems provokes additional power quality problems in the form of frequency and voltage fluctuations, due to rapidly changing nature of the wind [1–3].

The existing method used to solve these problems involves installation of batteries. The batteries are however constrained by their load cycles. There are some environmental concerns related to battery storage due to toxic gas generation during battery charge/discharge operation. The disposal of hazardous materials presents some disposal problems. On the other hand, the technical improvements in SMES and a better knowledge of dealing with cryogenic systems have made the SMES units to penetrate the market very fast [4–7]. The dynamic performance of an SMES system is far superior to other storage technologies. The shorter response time is the leading advantage and at the same time, system operation and life time are not influenced by the number of duty cycles or the depth of discharge as is the case for classical batteries. The estimated life of a typical SMES system is about 30 years. With the on going fast evolution in power electronics and SMES technology the estimated cost within 10 years is expected to be almost 25% of present cost. SMES systems are compact, self-contained and highly mobile. They contain no hazardous chemicals, produce no flammable gases and can be kept at remote locations. The SMES unit can be controlled to produce both active and reactive power modulations in the four quadrants of the P–Q plane. It can thus be concluded that the SMES system therefore perfectly fits the wind-diesel system for power quality improvement.

To exchange the real and reactive powers between the SMES unit and an ac bus of the wind-diesel power system suitable control strategies are required. The parameters of a wind-diesel

* Corresponding author. Tel.: +91 9419501253; fax: +91 1942420475.
E-mail address: sadial_14@yahoo.com (S.A. Lone).

0378-7753/$ – see front matter © 2006 Elsevier B.V. All rights reserved.
doi:10.1016/j.jpowsour.2006.09.004

Nomenclature

$E_{d''}$, $E_{q''}$ synchronous generator voltage behind subtransient reactances
E'_D, E'_Q real and imaginary components of induction machine voltage behind transient reactance(p.u.)
E_{fd} synchronous generator field voltage (p.u.)
$E_{q'}$ synchronous generator voltage behind transient reactance (p.u.)
f frequency(Hz) at load bus/wind park bus
H_A total wind turbine and wind generator inertia constant (s)
I_d, I_q direct and quadrature axis components of synchronous machine injected current
I_D, I_Q direct and quadrature axis components of induction machine injected current
$I_{Dsm}I_{Qsm}$ D–Q components of SMES current
I_{sm} current supplied by SMES
I^0_{sm} nominal current of SMES coil
L_{sm} SMES coil inductance
P_{dem} real power demanded by SMES unit
P_{sm} real power supplied by SMES unit
$P_{sm'}$ real power inputted to SMES unit
Q_{dem} reactive power demanded by SMES unit
Q_{sm} reactive power supplied by SMES unit
$Q_{sm'}$ reactive power inputted to SMES unit
$r_{s1} = r_{s2}$ stator resistance of synchronous machine (p.u.)
r_{s3} stator resistance of induction machine (p.u.)
S induction machine slip
T_{Ae} electromagnetic torque developed by induction machine (p.u.)
T_{Am} mechanical torque developed by wind turbine (p.u.)
T_{dc} converter time delay
T_{De} Electromagnetic torque developed by synchronous machine (p.u.)
T_{Dm} mechanical torque developed by diesel engine (p.u.)
T'_0 Induction generator rotor open circuit time constant (s)
V_d, V_q direct and quadrature axis components of synchronous machine terminal voltage (p.u.)
V_D, V_Q real and imaginary components of induction machine terminal voltage (p.u.)
V_{sm} SMES coil voltage
V^0_{sm} dc voltage of each converter with firing anglr equal to zero
$|V|$ magnitude of voltage of induction generator bus/load bus (p.u.)
X induction generator open circuit reactance (p.u.)
X' induction generator open circuit transient reactance (p.u.)
X_d, X_q synchronous generator reactance of direct and quadrature axis(p.u.)
X'_d, X'_q synchronous generator transient reactance of direct and quadrature axis (p.u.)
X''_d, X''_q synchronous generator subtransient reactance of direct and quadrature axis (p.u.)

Greek letters
ω_A wind generator angular velocity (p.u.)
ω_0 synchronous angular velocity

power system change with operating conditions. Thus, the best performance cannot be achieved by fixed gain controllers. To improve the performance of a wind-diesel power system for different operating conditions, self-tuning controllers were proposed [8]. A major disadvantage of the self-tuning control scheme is the need to identify system model parameters in real time, which is very time consuming. In order to get rid of the computational burden associated with self-tuning control, a different control strategy based on fuzzy logic is proposed, in this paper. The advantage with the fuzzy logic controllers is their ability to effect non-linear control actions, which are desirable for better system dynamic performance. There is no need for parameter identification and these controllers are less dependent on rigorous mathematical models. The proposed fuzzy logic control scheme is very simple and has a small number of rules. The input signals for this scheme are SMES coil current, frequency and voltage deviations at wind park bus/load bus. Various models are developed for various perturbations and system configurations. The effect of associating the SMES unit with the wind-diesel system is then investigated using simulation studies. In one of the configurations of the hybrid system, the SMES unit is connected to load bus and the performance of this configuration is compared with that of another case in which the SMES unit is connected to wind park bus.

2. System under study

Fig. 1 shows the system under study [9], which consists of two synchronous machines driven by diesel engines, ten induction machines driven by stall regulated wind turbines, transmission network, capacitor banks and a load. In one of the system configurations, the proposed SMES is connected to the wind park bus while in another configuration it interacts with the wind-diesel system through the load bus.

3. Description of system components

3.1. Wind turbine

Each stall regulated wind turbine and its coupled induction generator is represented by a lumped single mass, so that equation of motion can be written as:

$$\frac{d}{dt}(\omega_A) = \frac{1}{H_A}(T_{Am} - T_{Ae}) \quad (1)$$

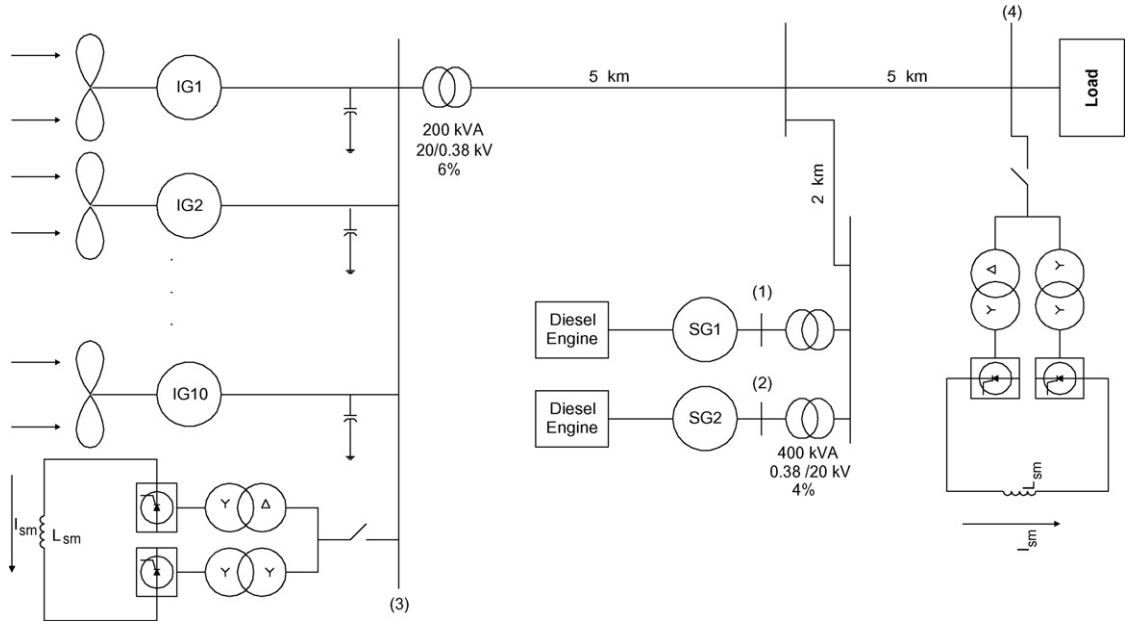

Fig. 1. Wind-diesel–SMES System.

3.2. Induction generators

Each induction machine coupled to a wind turbine is an asynchronous machine operating with a negative slip and electromagnetic torque. The model of each machine in synchronously rotating (D–Q) reference frame is expressed as:

Stator equations (in p.u.):

$$V_{\mathrm{D}} = E'_{\mathrm{D}} + r_{\mathrm{s3}} I_{\mathrm{D}} - X' I_{\mathrm{Q}} \tag{2}$$

$$V_{\mathrm{Q}} = E'_{\mathrm{Q}} + r_{\mathrm{s3}} I_{\mathrm{Q}} + X' I_{\mathrm{D}} \tag{3}$$

Rotor equations (in p.u.):

$$\frac{\mathrm{d}}{\mathrm{d}t}(E'_{\mathrm{D}}) = \frac{1}{T'_0}[-E'_{\mathrm{D}} - (X - X')I_{\mathrm{Q}}] + S\omega_0 E'_{\mathrm{Q}} \tag{4}$$

$$\frac{\mathrm{d}}{\mathrm{d}t}(E'_{\mathrm{Q}}) = \frac{1}{T'_0}[-E'_{\mathrm{Q}} - (X - X')I_{\mathrm{D}}] + S\omega_0 E'_{\mathrm{D}} \tag{5}$$

Electromagnetic torque equation:

$$T_{\mathrm{Ae}} = E'_{\mathrm{D}} I_{\mathrm{D}} + E'_{\mathrm{Q}} I_{\mathrm{Q}} \tag{6}$$

3.3. Capacitor compensation

For the induction generator, driven by a wind turbine, it is a well-known fact that it can deliver only active power and requires reactive power from the grid. The requirement can be quite significant even at no-load. The induction generator has a reactive power requirement, which varies with active power generated by it. In this paper, the 75% of the reactive power requirement is compensated with the shunt capacitors and the remaining portion of the reactive power requirement is drawn from the network. The capacitor banks installed for compensation of reactive power demanded by induction machines are modeled by incorporating their equivalent reactance value in the network admittance matrix.

3.4. Synchronous machines and their associated devices

Each synchronous machine driven by a diesel engine unit is represented by voltage and torque equations in machine (d–q) reference frame as:

Stator equations (in p.u.):

$$V_{\mathrm{d}} = E''_{\mathrm{d}} - r_{si} I_{\mathrm{d}} - X''_{\mathrm{q}} I_{\mathrm{q}} \tag{7}$$

$$V_{\mathrm{q}} = E''_{\mathrm{q}} - r_{si} I_{\mathrm{q}} - X''_{\mathrm{d}} I_{\mathrm{d}} \tag{8}$$

$(i = 1, 2)$

Rotor equations (in p.u.):

$$\frac{\mathrm{d}}{\mathrm{d}t}(E''_{\mathrm{d}}) = -\frac{1}{T''_{\mathrm{q0}}}[E''_{\mathrm{d}}(X_{\mathrm{q}} - X''_{\mathrm{q}})I_{\mathrm{q}}] \tag{9}$$

$$\frac{\mathrm{d}}{\mathrm{d}t}(E'_{\mathrm{q}}) = \frac{1}{T'_{\mathrm{d0}}}\left[E_{\mathrm{fd}} - \frac{X_{\mathrm{d}} - X''_{\mathrm{d}}}{X'_{\mathrm{d}} - X''_{\mathrm{d}}}E'_{\mathrm{q}} + \frac{X_{\mathrm{d}} - X'_{\mathrm{d}}}{X'_{\mathrm{d}} - X''_{\mathrm{d}}}E''_{\mathrm{q}}\right] \tag{10}$$

$$\frac{\mathrm{d}}{\mathrm{d}t}(E''_{\mathrm{q}}) = -\frac{1}{T''_{\mathrm{d0}}}[E''_{\mathrm{q}} - E'_{\mathrm{q}} + (X'_{\mathrm{d}} - X''_{\mathrm{q}})I_{\mathrm{d}}] \tag{11}$$

Electromagnetic torque equation is:

$$T_{\mathrm{De}} = E''_{\mathrm{d}} I_{\mathrm{d}} + E''_{\mathrm{q}} I_{\mathrm{q}} - (X''_{\mathrm{d}} - X''_{\mathrm{q}})I_{\mathrm{d}} I_{\mathrm{q}} \tag{12}$$

The standard models are used for the diesel engines and their associated speed governors [8,9]. The AVRs used are of IEEE type1 [8,9].

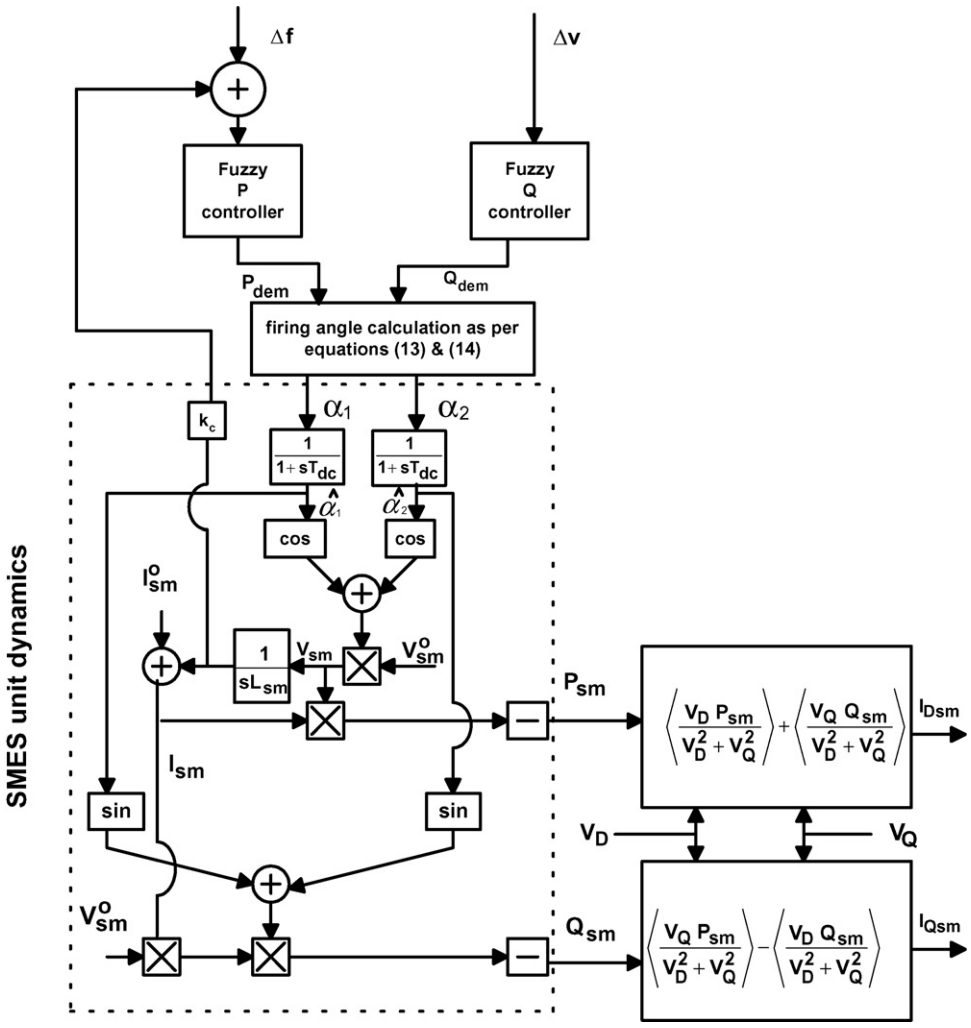

Fig. 2. SMES unit dynamics and control.

3.5. Transmission network

With the transmission line characteristics (R_T, X_T) per unit length known, they could be multiplied by the line length [8,9] and the resulting values considered concentrated over transmission line.

3.6. Load

In a particular configuration, the connected load is represented by a constant admittance and its admittance value is incorporated in the network admittance matrix.

3.7. SMES system

The various forcing functions (perturbations) in a wind-diesel system upset the real and reactive power balance and thus affect the system frequency and voltage. Before the diesel engine governors and AVRs will act, a control device like SMES which is capable of modulating fast, the active and reactive powers is an appropriate candidate for power quality improvement of the system. When a superconducting coil is connected through a GTO/IGBT based, 12-pulse converter to a three-phase ac bus, it can modulate real and reactive powers. The control of the firing angles α_1 and α_2 of the cascaded six-pulse converters gives the SMES unit capability to exchange (inject/absorb) active and reactive powers, independently with the system [7]. For initial charging of the SMES coil the converter voltage is held positive at a suitable constant value. When the inductor current reaches its nominal value $I^0_{sm,}$ the SMES unit is connected to wind park/load bus and left floating by adjusting α_1 to 90°, α_2 to 270°. Under these conditions, there is no exchange of real and reactive powers between the SMES unit and the wind-diesel system. As soon as the controllers associated with the SMES unit experience a change in voltage and frequency at the bus SMES unit is connected to the wind-diesel system, the firing angles of the converters are controlled to modulate active and reactive powers. The block diagram of Fig. 2 depicts the modeling and the control of SMES unit. Details about this block diagram are given in the following sub sections.

3.7.1. Fuzzy logic controllers for SMES

Two fuzzy logic controllers, P- and Q-controller generate, P_{dem} and Q_{dem}, which represent, respectively, the active and

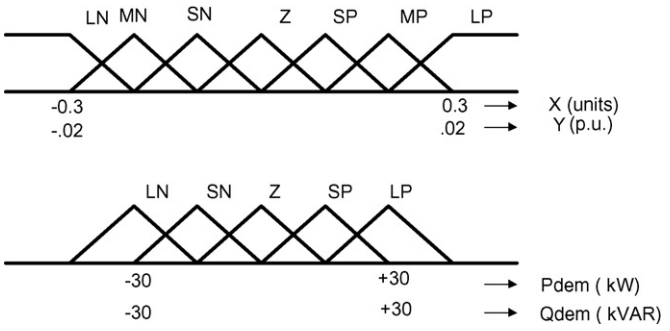

Fig. 3. Membership functions for P and Q controllers.

reactive powers required to be supplied from the SMES system. The P-controller uses a mixture of ac bus frequency deviation and SMES coil current deviation signals. For continuous control, it is necessary that SMES coil current has a tendency to attain its nominal value, that is why an appropriate portion of this signal is added to frequency deviation signal. The Q-controller on the other hand requires the ac bus voltage deviation for generating Q_{dem}. Triangular type of membership functions are used for input as well as output fuzzy sets as shown in Fig. 3. For the P-controller, the universe for discourse for the input (X) units and output P_{dem} are chosen as (−0.3 units, +0.3 units) and (−30 kW, +30 kW), respectively. For Q-controller, the universe of discourse for input (Y) units and the output Q_{dem} are chosen as (−0.02 p.u. and +0.02 p.u) and (−30 kVAR, +30 kVAR), respectively. The fuzzy rules are determined from Table 1. Seven fuzzy sets are considered for input variables and five sets for output variables and the height defuzzification method is used for computing control signals.

3.7.2. Calculation of firing angles

The firing angles of two cascaded six-pulse converters under four-quadrant operation are calculated from P'_{dem} (=$-P_{dem}$) and Q'_{dem} (=$-Q_{dem}$) as per the following equations [7]:

$$\alpha_1 = \cos^{-1}\left\langle \frac{P'_{dem}}{\sqrt{P'^2_{dem} + Q'^2_{dem}}} \right\rangle + \cos^{-1}\left\langle \frac{\sqrt{P'^2_{dem} + Q'^2_{dem}}}{2V^o_{sm} I_{sm}} \right\rangle \quad (13)$$

$$\alpha_2 = \cos^{-1}\left\langle \frac{P'_{dem}}{\sqrt{P'^2_{dem} + Q'^2_{dem}}} \right\rangle - \cos^{-1}\left\langle \frac{\sqrt{P'^2_{dem} + Q'^2_{dem}}}{2V^o_{sm} I_{sm}} \right\rangle \quad (14)$$

Table 1
Rule base for active/reactive power generators

X or Y	LN	MN	SN	Z	SP	MP	LP
P_{dem} or Q_{dem}	LP	LP	SP	Z	SN	LN	LN

3.7.3. SMES unit dynamics

The actual values of active and reactive powers, P_{sm} and Q_{sm}, injected by SMES at the ac bus are calculated after taking into account the converter delay and the SMES dynamics presented in Fig. 2. In this figure, the outputs of the blocks representing the converter delay are identified as $\hat{\alpha}_1$ and $\hat{\alpha}_2$. The various equations governing the SMES unit are then.

Voltage across the SMES coil

$$V_{sm} = V^0_{sm}(\cos\hat{\alpha}_1 + \cos\hat{\alpha}_2) \quad (15)$$

Current through the SMES coil

$$I_{sm} = \frac{1}{L_{sm}}\int_{t_0}^{t} V_{sm}\,d\tau + I^0_{sm} \quad (16)$$

Active power injected by SMES unit at ac bus

$$P_{sm} = -V^0_{sm} I_{sm}(\cos\hat{\alpha}_1 + \cos\hat{\alpha}_2) \quad (17)$$

Reactive power injected by SMES at ac bus

$$Q_{sm} = -V^0_{sm} I_{sm}(\sin\hat{\alpha}_1 + \sin\hat{\alpha}_2) \quad (18)$$

Once these equations are cast in the block diagram form, the middle portion of Fig. 2 (labeled as SMES unit dynamics) is obtained.

3.7.4. SMES unit model in D–Q rotating frame

The D and Q components of the current injected by SMES unit at the ac bus, in response to calculated firing angles α_1 and α_2, are calculated as per the following equations:

$$I_{Dsm} = \left\langle \frac{V_D P_{sm}}{V_D^2 + V_Q^2} \right\rangle + \left\langle \frac{V_Q Q_{sm}}{V_D^2 + V_Q^2} \right\rangle \quad (19)$$

$$I_{Qsm} = \left\langle \frac{V_Q P_{sm}}{V_D^2 + V_Q^2} \right\rangle - \left\langle \frac{V_D Q_{sm}}{V_D^2 + V_Q^2} \right\rangle \quad (20)$$

In Eqs. (19) and (20), V_D and V_Q are D–Q components of ac bus voltage, where SMES is connected. The complete SMES unit dynamics and control scheme is given in Fig. 2. In this figure, K_c represents the SMES coil current feedback gain the importance of which is already given in Section 3.7.1.

4. Compact network-machine model

In general, the network equations for the hybrid wind-diesel SMES system can be written as:

$$\underline{I} = [Y_{Bus}]\underline{V} \quad (21)$$

where $[Y_{Bus}]$ is the admittance matrix of the system, formulated with equivalent admittances of the capacitor banks, transformers, and loads incorporated. In the partitioned form, the Eq. (21) can be written as:

$$\begin{bmatrix} \underline{I_n} \\ \underline{0} \end{bmatrix} = \begin{bmatrix} [Y_{nn}] & [Y_{nr}] \\ [Y_{rn}] & [Y_{rr}] \end{bmatrix} \begin{bmatrix} \underline{V_n} \\ \underline{V_r} \end{bmatrix} \quad (22)$$

where subscript n denotes the total number of network nodes at which (synchronous and induction) generators and SMES unit

are connected. The subscript r on the other hand denotes the remaining nodes. The above equation can be simplified to take the form of (23)

$$\underline{V_n} = \lfloor Z_{TT} \rfloor \underline{I_n} \tag{23}$$

where

$$[Z_{TT}] = [Y_{TT}]^{-1} \quad \text{and} \quad [Y_{TT}] = ([Y_{nn}] - [Y_{nr}][Y_{rr}]^{-1}[Y_{rn}])$$

Using node elimination method we retain only the buses where synchronous and induction machines are connected and eliminate the rest of the buses. For various cases, the compact models are developed in the following sub sections.

4.1. SMES at wind park bus

In D–Q component form, one can write Eq. (23) as:

$$\lfloor V_{1DQ} \rfloor = \lfloor GB_{1DQ} \rfloor \lfloor I_{1DQ} \rfloor + \lfloor GB_{1DQ} \rfloor \lfloor I_{1DQSM} \rfloor \tag{24}$$

where:

$$[V_{1DQ}] = [\, V_{D1} \quad V_{Q1} \quad V_{D2} \quad V_{Q2} \quad V_{D3} \quad V_{Q3} \,]^T$$

$$[I_{1DQ}] = [\, I_{D1} \quad I_{Q1} \quad I_{D2} \quad I_{Q2} \quad I_{D3} \quad I_{Q3} \,]^T$$

$$[I_{1DQSM}] = [\, 0 \quad 0 \quad 0 \quad 0 \quad I_{DSM} \quad I_{QSM} \,]^T$$

Elements of GB_{1DQ} are given in Appendix A.

Eq. (24) can be combined with the stator equations of the synchronous and induction machines to obtain a compact model. For the sake of simplicity, all the induction machines can be represented by a single equivalent induction machine run by a single turbine [9,10], on the assumption that all wind machines operate under same wind conditions. After transforming synchronous machine equations to D–Q axis, we obtain the compact model of Eq. (25).

$$I_{1\underline{DQ}} = [H_{1DQ}]^{-1}[E_{1DQ} - [GB_{1DQ}]I_{1\underline{DQSM}}] \tag{25}$$

where, the elements of $[GB_{1DQ}]$ and that of $[H_{1DQ}]$ are given in Appendix A and

$$I_{1\underline{DQ}} = [I_{D1} \;\; I_{Q1} \;\; I_{D2} \;\; I_{Q2} \;\; I_{D3} \;\; I_{Q3}]^T$$

$$E_{1DQ} = [\, E''_{D1} \quad E''_{Q1} \quad E''_{D2} \quad E''_{Q2} \quad E'_{D3} \quad E'_{Q3} \,]^T$$

$$I_{1DQSM} = [\, 0 \quad 0 \quad 0 \quad 0 \quad I_{DSM} \quad I_{QSM} \,]^T$$

4.2. SMES at load bus

In D–Q (synchronously rotating reference frame) component form, for this case, one can write Eq. (23) as:

$$\lfloor V_{2DQ} \rfloor = \lfloor GB_{2DQ} \rfloor \lfloor I_{2DQ} \rfloor + \lfloor GB_{3DQ} \rfloor \lfloor I_{2DQSM} \rfloor \tag{26}$$

where

$$[V_{2DQ}] = [\, V_{D1} \quad V_{Q1} \quad V_{D2} \quad V_{Q2} \quad V_{D3} \quad V_{Q3} \,]^T$$

$$[I_{2DQ}] = [\, I_{D1} \quad I_{Q1} \quad I_{D2} \quad I_{Q2} \quad I_{D3} \quad I_{Q3} \,]^T$$

$$[I_{2DQSM}] = [\, I_{DSM} \quad I_{QSM} \,]^T$$

Elements of GB_{2DQ} and $[GB_{3DQ}]$ are given in Appendix A.

Eq. (26) can be combined with the stator equations of the synchronous and induction machines as in previous case to obtain a compact model of Eq. (27).

$$I_{2\underline{DQ}} = [H_{2DQ}]^{-1}[E_{2DQ} - GB_{3DQ}]I_{2DQSM} \tag{27}$$

The elements of H_{2DQ} are given in Appendix A.

$$[I_{2\underline{DQ}}] = [\, I_{D1} \quad I_{Q1} \quad I_{D2} \quad I_{Q2} \quad I_{D3} \quad I_{Q3} \,]^T$$

$$[E_{2\underline{DQ}}] = [\, E''_{D1} \quad E''_{Q1} \quad E''_{D2} \quad E''_{Q2} \quad E'_{D3} \quad E'_{Q3} \,]^T$$

$$[I_{2\underline{DQSM}}] = [\, I_{DSM} \quad I_{QSM} \,]^T$$

4.3. Wind park disconnection when SMES is at wind park bus

In this case, we have,

$$\lfloor V_{3DQ} \rfloor = \lfloor GB_{4DQ} \rfloor \lfloor I_{3DQ} \rfloor \lfloor GB_{5DQ} \rfloor \lfloor I_{3DQSM} \rfloor \tag{28}$$

where

$$[V_{3DQ}] = [\, V_{D1} \quad V_{Q1} \quad V_{D2} \quad V_{Q2} \,]^T$$

$$[I_{3DQ}] = [\, I_{D1} \quad I_{Q1} \quad I_{D2} \quad I_{Q2} \,]^T$$

$$[I_{3DQSM}] = [\, I_{DSM} \quad I_{QSM} \,]^T$$

Elements of GB_{4DQ} and GB_{5DQ} are given in Appendix A.

The final compact model for this case is given by Eq. (29)

$$I_{3\underline{DQ}} = [H_{3DQ}]^{-1}[E_{3DQ} - [GB_{4DQ}]I_{3DQSM}] \tag{29}$$

The elements of $[H_{3DQ}]$ and are given in Appendix A.

4.4. Wind park disconnection when SMES is at load bus

The model for this case is similar to the one obtained for Section 4.3.

5. Simulation studies

Based on the dynamic models of various components, presented in the previous section, MATLAB programs were developed and a range of simulations was performed. The behaviour of the system under various disturbances like wind park disconnection, turbulent wind, sudden wind power variation and load changes is examined. Before running the dynamic programs for a particular disturbance, the load flow and initial condition program files are run to obtain steady state data prior to the disturbance (henceforth $t < t_0$). The power system considered comprises of two identical diesel units, each of 240 kW capacity. The wind park comprises of 10 identical wind turbines coupled

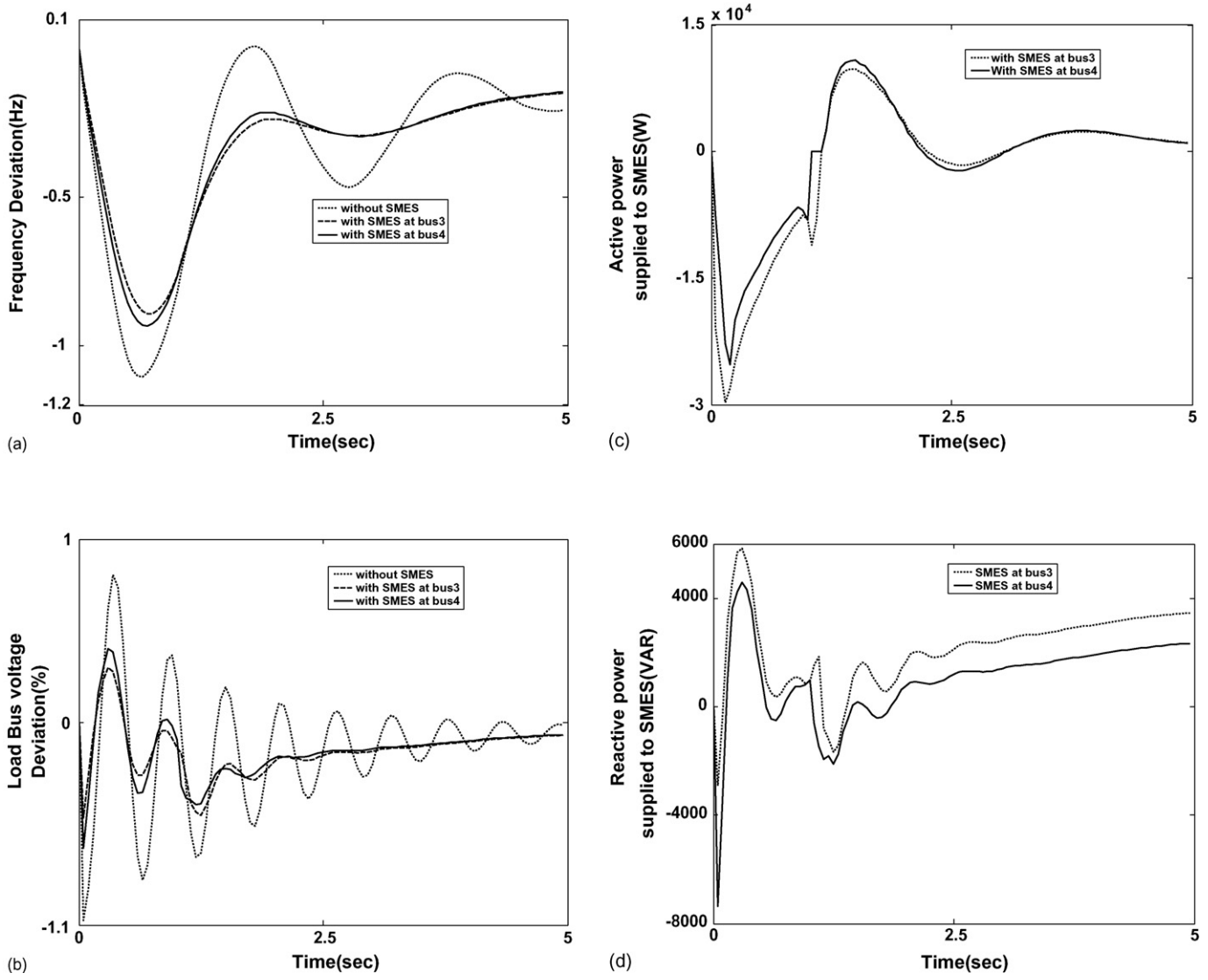

Fig. 4. (a) Frequency deviation (Hz) due to wind park disconnection, (b) voltage deviation at load bus (%) due to wind park disconnection, (c) active power supplied to SMES (W) and (d) reactive power supplied to SMES (VARS).

to asynchronous generators, each of 12 kW. The load demand varies between 150 and 360 kW. The SMES unit considered requires a peak energy storage of just a few kJ and its converter rating is about 5% of the overall system capacity.

The power quality results obtained with different configurations are compared for different cases. The SMES unit is first introduced at wind park bus and then shifted to load bus, to study the effect of the position of SMES unit, if any, on the power quality of the hybrid system.

5.1. Case1: wind park disconnection

The objective of this case study is to examine the behaviour of the power system with abrupt change in penetration level. Initially, the wind turbines are generating 100 kW and the power system load is 312 kW/200 kVAR, while the system frequency is 50 Hz. At $t = t_0$, the wind park along with associated capacitor banks is disconnected. According to Fig. 4(a and b), the power quality of the wind-diesel system is not acceptable [9].

For example the frequency deviation exceeds the acceptable limit of 1 Hz. The same figures reveal that with the introduction of SMES unit at wind park bus, the quality of the power supplied by the hybrid system is quite satisfactory. However, as revealed by the simulation results, power quality is not improved further as SMES unit is shifted from wind park bus to load bus. Fig. 4(c and d) shows active and reactive power supplied by SMES. The variations in these variables are due to continuous interaction of the SMES unit with the system during transients.

5.2. Case 2: operation under turbulent wind

The objective of this case study is to examine the behaviour of the hybrid power system when the wind turbines operate in turbulent wind. This mode of operation is very common for wind power based power systems.

Initially, the wind turbines are supplying 50 kW of power and the load on the power system is taken as 260 kW/182 kVAR. For $t > t_0$, the wind turbines operate in turbulent wind mode and

the power supplied by the wind turbines varies as shown in Fig. 5(a).

Fig. 5(b and c) depicts the power quality results of the power system under consideration under turbulent wind operation. Although, for the wind-diesel system the maximum deviations in frequency and voltage are within limits, so is not the case with rate of change of these variables [9]. This rate of change is an additional criterion for acceptable operation of power systems with wind energy conversion systems. For example, a high rate of change of voltages causes unacceptable flicker even if the maximum variation is in the neighbourhood of 2% [8,9]. Thus, the power quality of the wind-diesel system is not satisfactory for turbulent wind. The simulation results clearly establish the effect of introducing the SMES unit, on the power quality under most common mode of wind turbine operation. It can be inferred from the results that with the introduction of SMES unit, the maximum deviations in system frequency and voltage are reduced to some extent. Although the power quality with SMES is satisfactory, the rate of change in load bus voltage is not reduced to a great extent because the fuzzy logic control proposed in this paper does not make use of rate of change of load bus voltage as one of the input variables.

5.3. Case 3: operation under sudden wind power changes

In this case study, the behaviour of the wind-diesel power system under step wind changes is studied. The wind power is considered to contain also a small stochastic component in the study. The stochastic component was generated by using MATLAB/SIMULINK toolbox and was then added to step wind changes thus resulting wind power profile of Fig. 6(a).

For $t < t_0$ the wind turbines are supplying 50 kW of power and the load is 260 kW/182 kVAR. For $t > t_0$ the system operates in the wind power profile of Fig. 6(a). The simulation results for this mode of operation are shown in Fig. 6(b and c). These figures clearly show the positive impact of proposed control scheme on the power quality of the system, under sudden wind power changes.

5.4. Case 4: load changes

Change in load is a noteworthy source of perturbation in stand-alone power systems. This is because of the fact that a stand-alone power system has low inertia and is not able to contain the variations in system frequency and voltage unlike the utility grid. A change in static load is modeled as a change in network topology.

Two different cases were studied as indicated in Tables 2 and 3. In one case, active power load changes are considered while in second case the active as well as reactive power load

Table 2
Load profile for active power load disturbance

Time (s)	Active power (kW)	Reactive power (kW)
$t < 0$	260	182
$0 < t \leq 10$	360	182

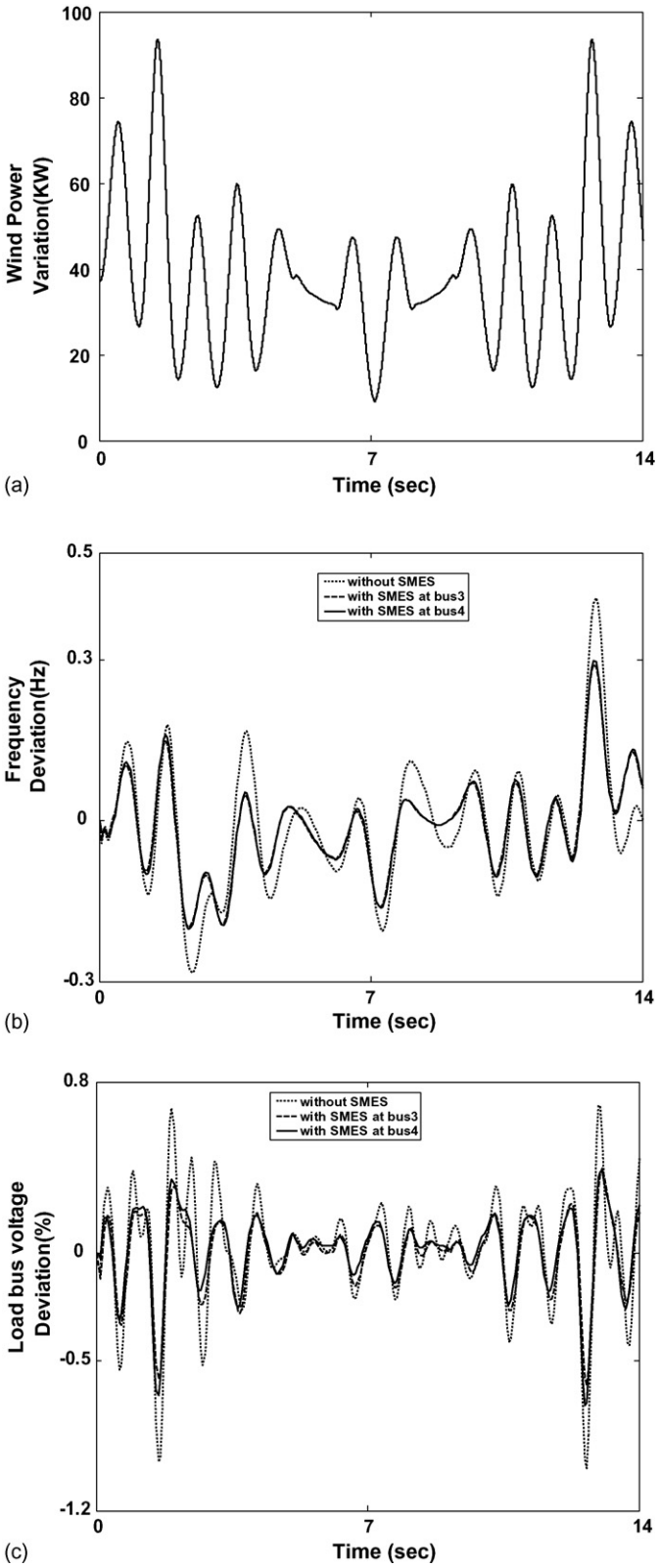

Fig. 5. (a) Wind power variation (kW), (b) frequency deviation (Hz) due to turbulent wind and (c) voltage deviation at load bus (%) due to turbulent wind.

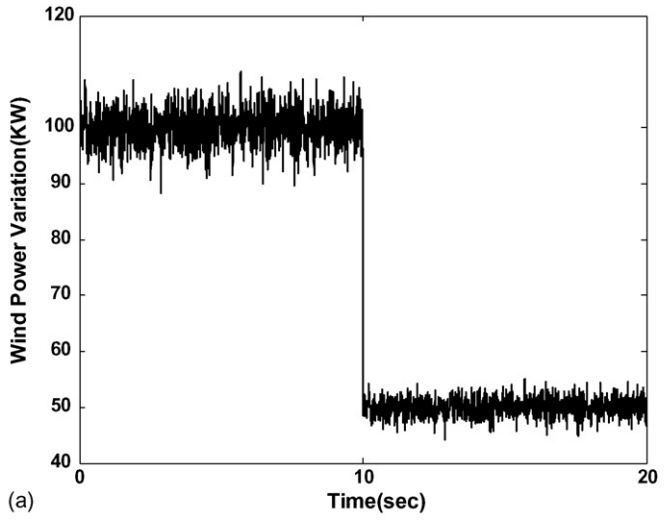

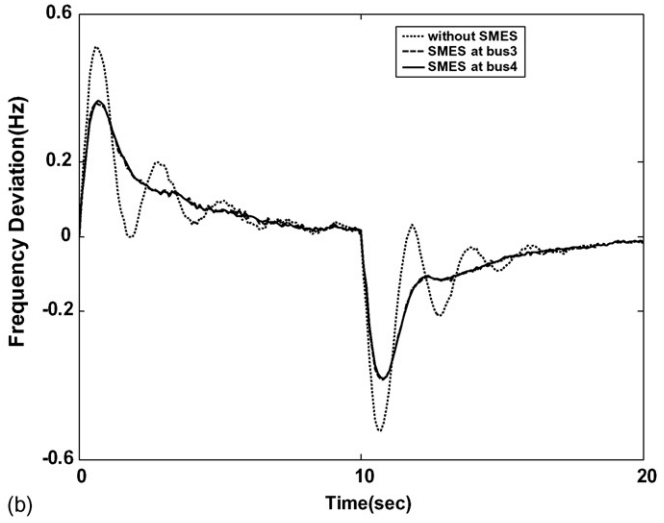

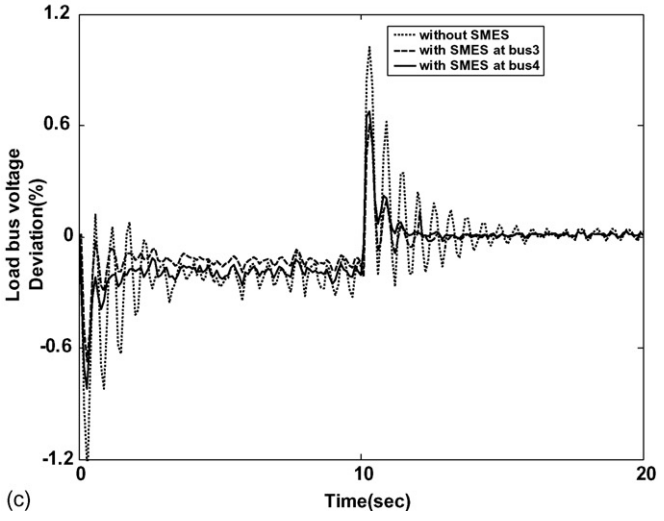

Fig. 6. (a) Stochastic wind power variation (kW), (b) frequency deviation (Hz) due to stochastic wind disturbance and (c) voltage deviation at load bus (%) due to stochastic wind disturbance.

Table 3
Load profile for active/reactive power load disturbance

Time (s)	Active power (kW)	Reactive power (kW)
$t<0$	260	182
$0<t\leq 10$	360	200

changes are considered. For $t<t_0$, the power supplied by the wind turbines is 50 kW and the load on the system is 260 kW/182 kVAR. In both the cases, wind power is considered constant.

The simulation results pertaining to these two cases are depicted in Figs 7(a and b) and 8(a and b), respectively. It is observed from these results that the association of SMES unit with the wind-diesel system helps in maintaining the power quality in this case also.

In none of the case studies, the SMES coil current exceeds 500A. Thus an SMES unit with a peak-stored energy of just

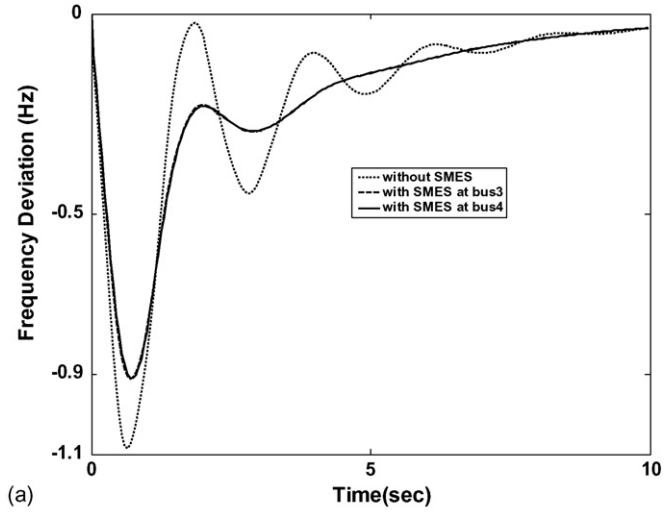

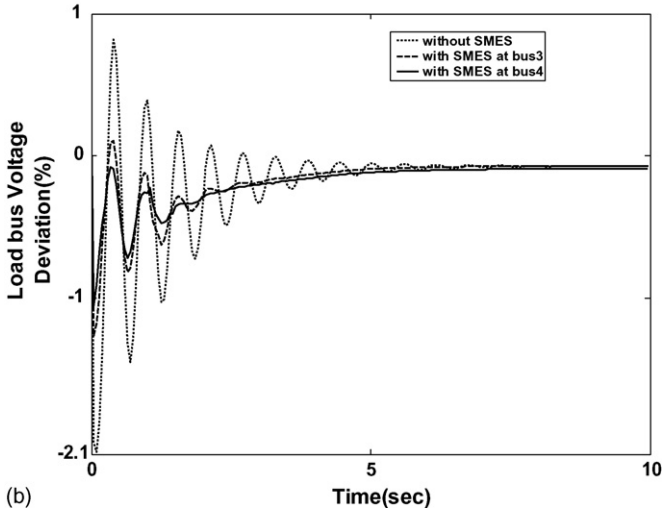

Fig. 7. (a) Frequency deviation (Hz) due to active power load disturbance and (b) voltage deviation at load bus (%) due to active power load disturbance.

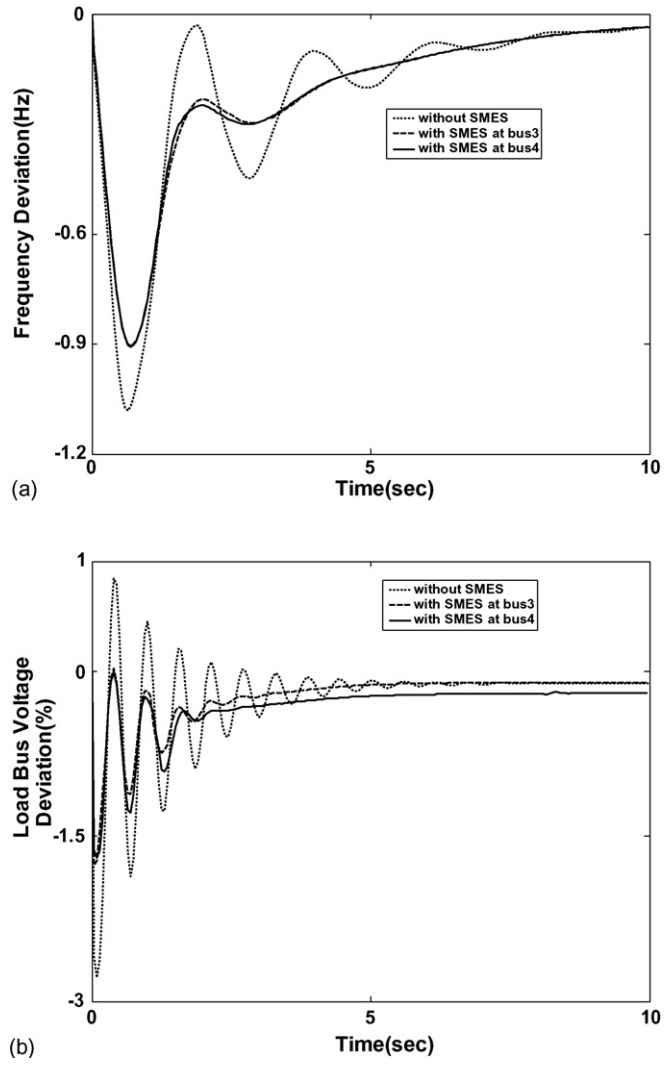

Fig. 8. (a) Frequency deviation (Hz) due to active and reactive power load disturbance and (b) voltage deviation (%) due to active and reactive power load disturbance.

a few kJ is sufficient to deal with all these disturbances. The examination of active and reactive power curves of the SMES unit reveal that the SMES converter rating required is just 5% of the overall system capacity.

6. Conclusions

An effective control scheme, based on SMES unit, for power quality improvement of a typical multimachine wind-diesel power system is proposed. The effect of insertion of SMES unit at two alternative places is explored. Complete models for various configurations and case studies are developed. The SMES unit is operated in four quadrants using a fuzzy logic control strategy. The proposed scheme is investigated for its impact on the system performance for various disturbances like wind park disconnection, wind gusts, abrupt wind changes and load perturbations. The simulation results show that the proposed scheme helps to maintain the power quality of the system, within the limits, for various perturbations. The simulation results also reveal that the quality of power is not improved much as the SMES unit is shifted from wind-park bus to the load bus.

Appendix A

A.1. System data

Base power 400 kVA for the whole system.

A.2. Synchronous generators

Nominal power (kW) = 240, nominal voltage = 380 V.

Nominal apparent power (kVA) = 240, $r_s = 0.067$, $X_d = 260\%$, $X_q = 156$, $X'_d = 22\%$, $X''_d = 15\%$, $X''_q = 22.5\%$, $T'_{do} = 1.182$ s, $T''_{do} = 0.015$ s, $T''_{qo} = 1.18$ s.

A.3. Induction generators

Nominal power (kW) = 12, nominal voltage = 380 V, nominal speed = 1545 rpm, $r_s = 0.022$ p.u., $x_s = 0.181$ p.u, $x_m = 1.605$ p.u., $r_r = 0.022$ p.u., $x_r = 0.181$ p.u., $H_A = 0.259$ s.

A.4. SMES

$L_{sm} = 0.264$ H, $I^0_{sm} = 350$ A, $V^0_{sm} = 42.5|V|$, $K_c = 0.01$

Elements of GB_{1DQ} are given by

$$[GB_{1DQ}] = \begin{bmatrix} G1_{11} & -B1_{11} & G1_{12} & -B1_{12} & G1_{13} & -B1_{13} \\ B1_{11} & G1_{11} & B1_{12} & G1_{12} & B1_{13} & G1_{13} \\ G1_{21} & -B1_{21} & G1_{22} & -B1_{22} & G1_{23} & -B1_{23} \\ B1_{21} & G1_{21} & B1_{22} & G1_{22} & B1_{23} & G1_{23} \\ G1_{31} & -B1_{31} & G1_{32} & -B1_{32} & G1_{33} & -B1_{33} \\ B1_{31} & G1_{31} & B1_{32} & G1_{32} & B1_{33} & G1_{33} \end{bmatrix}$$

Elements of $[H_{1DQ}]$

$$H_{1DQ}(1,1) = r_{s1} + (X''_{d1} - X''_{q1}) \sin\delta_1 \cos\delta_1 + G1_{11}$$
$$H_{1DQ}(1,2) = -(X''_{q1} \sin^2\delta_1 + X''_{d1} \cos^2\delta_1 + B1_{11})$$
$$H_{1DQ}(1,3) = G1_{12}$$
$$H_{1DQ}(1,4) = -B1_{12}$$
$$H_{1DQ}(1,5) = G1_{13}$$
$$H_{1DQ}(1,6) = -B1_{13}$$
$$H_{1DQ}(2,1) = X''_{q1} \cos^2\delta_1 + X''\delta_1 \sin^2\delta_1 + B1_{11}$$
$$H_{1DQ}(2,2) = r_{s1} + (X''_{q1} - X''_{d1}) \sin\delta_1 \cos\delta_1 + G1_{11}$$
$$H_{1DQ}(2,3) = B1_{12}$$
$$H_{1DQ}(2,4) = G1_{12}$$
$$H_{1DQ}(2,5) = B_{113}$$
$$H_{1DQ}(2,6) = G1_{13}$$
$$H_{1DQ}(3,1) = G1_{21}$$
$$H_{1DQ}(3,2) = -B1_{21}$$
$$H_{1DQ}(3,3) = r_{s2} + (X''_{d2} - X''_{q2}) \sin\delta_2 \cos\delta_2 + G1_{22}$$
$$H_{1DQ}(3,4) = -(X''_{q2} \sin^2\delta_2 + X''_{d2} \cos^2\delta_2 + B1_{22})$$
$$H_{1DQ}(3,5) = G1_{23}$$
$$H_{1DQ}(3,6) = -B1_{23}$$
$$H_{1DQ}(4,1) = B1_{21}$$
$$H_{1DQ}(4,2) = G1_{21}$$
$$H_{1DQ}(4,3) = X''_{q2} \cos^2\delta_2 + X''_{d2} \sin^2\delta_2 + B1_{22}$$
$$H_{1DQ}(4,4) = r_{s2} + (X''_{q2} - X''_{d2}) \sin\delta_2 \cos\delta_2 + G1_{22}$$
$$H_{1DQ}(4,5) = B_{123}$$
$$H_{1DQ}(4,6) = G1_{23}$$
$$H_{1DQ}(5,1) = G1_{31}$$
$$H_{1DQ}(5,2) = -B1_{31}$$
$$H_{1DQ}(5,3) = G1_{32}$$
$$H_{1DQ}(5,4) = -B1_{32}$$
$$H_{1DQ}(5,5) = r_{s3} + G1_{33}$$
$$H_{1DQ}(5,6) = -(X'_3 + B1_{33})$$
$$H_{1DQ}(6,1) = B1_{31}$$
$$H_{1DQ}(6,2) = G1_{31}$$
$$H_{1DQ}(6,3) = B1_{32}$$
$$H_{1DQ}(6,4) = G1_{32}$$
$$H_{1DQ}(6,5) = X'_3 + B1_{33}$$
$$H_{1DQ}(6,6) = r_{s3} + G1_{33}$$

The elements of GB_{2DQ} and GB_{3DQ} are given by

$$[GB_{2DQ}] = \begin{bmatrix} G2_{11} & -B2_{11} & G2_{12} & -B2_{12} & G2_{13} & -B2_{13} \\ B2_{11} & G2_{11} & B2_{12} & G2_{12} & B2_{13} & G2_{13} \\ G2_{21} & -B2_{21} & G2_{22} & -B2_{22} & G2_{23} & -B2_{23} \\ B2_{21} & G2_{21} & B2_{22} & G2_{22} & B2_{23} & G2_{23} \\ G2_{31} & -B2_{31} & G2_{32} & -B2_{32} & G2_{33} & -B2_{33} \\ B2_{31} & G2_{31} & B2_{32} & G2_{32} & B2_{33} & G2_{33} \end{bmatrix}$$

$$[GB_{3DQ}] = \begin{bmatrix} G2_{14} & B2_{14} & G2_{24} & B2_{24} & G2_{34} & B2_{34} \\ -B2_{14} & G2_{14} & -B2_{24} & G2_{24} & -B2_{34} & G2_{34} \end{bmatrix}^T$$

Elements of $[H_{2DQ}]$

$$H_{2DQ}(1,1) = r_{s1} + (X''_{d1} - X''_{q1}) \sin\delta_1 \cos\delta_1 + G2_{11}$$
$$H_{2DQ}(1,2) = -(X''_{q1} \sin^2\delta_1 + X''_{d1} \cos^2\delta_1 + B2_{11})$$
$$H_{2DQ}(1,3) = G2_{12}$$
$$H_{2DQ}(1,4) = -B2_{12}$$
$$H_{2DQ}(1,5) = G2_{13}$$
$$H_{2DQ}(1,6) = -B2_{13}$$
$$H_{2DQ}(2,1) = X''_{q1} \cos^2\delta_1 + X''_{d1} \sin^2\delta_1 + B2_{11}$$
$$H_{2DQ}(2,2) = r_{s1} + (X''_{q1} - X''_{d1}) \sin\delta_1 \cos\delta_1 + G2_{11}$$
$$H_{2DQ}(2,3) = B2_{12}$$
$$H_{2DQ}(2,4) = G2_{12}$$
$$H_{2DQ}(2,5) = B2_{13}$$
$$H_{2DQ}(2,6) = G2_{13}$$
$$H_{2DQ}(3,1) = G2_{21}$$
$$H_{DQ}(3,2) = -B2_{21}$$
$$H_{2DQ}(3,3) = r_{s2} + (X''_{d2} - X''_{q2}) \sin\delta_2 \cos\delta_2 + G2_{22}$$
$$H_{2DQ}(3,4) = -(X''_{q2} \sin^2\delta_2 + X''_{d2} \cos^2\delta_2 + B2_{22})$$
$$H_{2DQ}(3,5) = G2_{23}$$
$$H_{2DQ}(3,6) = -B2_{23}$$
$$H_{2DQ}(4,1) = B2_{21}$$
$$H_{2DQ}(4,2) = G2_{21}$$
$$H_{2DQ}(4,3) = X''_{q2} \cos^2\delta_2 + X''_{d2} \sin^2\delta_2 + B2_{22}$$
$$H_{2DQ}(4,4) = r_{s2} + (X''_{q2} - X''_{d2}) \sin\delta_2 \cos\delta_2 + G2_{22}$$
$$H_{2DQ}(4,5) = B2_{23}$$
$$H_{2DQ}(4,6) = G2_{23}$$
$$H_{2DQ}(5,1) = G2_{31}$$
$$H_{2DQ}(5,2) = -B2_{31}$$
$$H_{2DQ}(5,3) = G2_{32}$$
$$H_{2DQ}(5,4) = -B2_{32}$$
$$H_{2DQ}(5,5) = r_{s3} + G2_{33}$$
$$H_{2DQ}(5,6) = -(X'_3 + B2_{33})$$
$$H_{2DQ}(6,1) = B2_{31}$$
$$H_{DQ}(6,2) = G2_{31}$$
$$H_{2DQ}(6,3) = B2_{32}$$
$$H_{2DQ}(6,4) = G2_{32}$$
$$H_{2DQ}(6,5) = X'_3 + B2_{33}$$
$$H_{2DQ}(6,6) = r_{s3} + G2_{33}$$

The elements of $[GB_{4DQ}]$ and $[GB_{5DQ}]$ are given by

$$[GB_{4DQ}] = \begin{bmatrix} G3_{11} & -B3_{11} & G3_{12} & -B3_{12} \\ B3_{11} & G3_{11} & B3_{12} & G3_{12} \\ G3_{21} & -B3_{21} & G3_{22} & -B3_{22} \\ B3_{21} & G3_{21} & B3_{22} & G3_{22} \end{bmatrix}$$

$$[GB_{5DQ}] = \begin{bmatrix} G3_{13} & B3_{13} & G3_{23} & B3_{23} \\ -B3_{13} & G3_{13} & -B3_{23} & G3_{23} \end{bmatrix}$$

Elements of $[H_{3DQ}]$ are given by

$$H_{3DQ}(1,1) = r_{s1} + (X''_{d1} - X''_{q1}) \sin\delta_1 \cos\delta_1 + G3_{11}$$
$$H_{3DQ}(1,2) = -(X''_{q1} \sin^2\delta_1 + X''_{d1} \cos^2\delta_1 + B3_{11})$$
$$H_{3DQ}(1,3) = G3_{12}$$
$$H_{3DQ}(1,4) = -B3_{12}$$
$$H_{3DQ}(2,1) = X''_{q1} \cos^2\delta_1 + X''_{d1} \sin^2\delta_1 + B3_{11}$$
$$H_{3DQ}(2,2) = r_{s1} + (X''_{q1} - X''_{d1}) \sin\delta_1 \cos\delta_1 + G3_{11}$$
$$H_{3DQ}(2,3) = B3_{12}$$
$$H_{3DQ}(2,4) = G3_{12}$$
$$H_{3DQ}(3,1) = G3_{21}$$
$$H_{3DQ}(3,2) = -B3_{21}$$
$$H_{3DQ}(3,3) = r_{s2} + (X''_{d2} - X''_{q2}) \sin\delta_2 \cos\delta_2 + G3_{22}$$
$$H_{3DQ}(3,4) = -(X''_{q2} \sin^2\delta_2 + X''_{d2} \cos^2\delta_2 + B3_{22})$$
$$H_{3DQ}(4,1) = B3_{21}$$
$$H_{3DQ}(4,2) = G3_{21}$$
$$H_{3DQ}(4,3) = X''_{q2} \cos^2\delta_2 + X''_{d2} \sin^2\delta_2 + B3_{22}$$
$$H_{3DQ}(4,4) = r_{s2} + (X''_{q2} - X''_{d2}) \sin\delta_2 \cos\delta_2 + G3_{22}$$

References

[1] P.D. Ladakakos, M.G. Ioannides, Wind Eng. 23 (6) (1999) 353–364.

[2] I. Nojima, I. Takano, Y. Sawada, The 27th Annual Conference of the IEEE Industrial Electronics Society, 2001, IECON' 01, vol. 2, 29 Nov–2 Dec (2001) pp. 1303–1308.

[3] H. Sharma, S. Islam, C.V. Nayar, T. Pryor, IEEE Power Engineering Society Winter Meeting 2000, vol. 1, 23–27 Jan (2000) pp. 499–504.

[4] S. Hutardo, G. Gostales, A. de Lara, N. Moreno, J.M. Carrasco, E. Galvan, J.A. Sanchez, L.G. Franquelo, A new power stabilization control system based on making use of mechanical inertia of a variable-speed wind turbine for stand-alone wind-diesel applications, in: IECON 02 Industrial Electronics society 28th Annual conference, vol. 4, 5–8 November, 2002, pp. 3326–3331.

[5] K.C. Seong, H.J. Kim, S.W. Kim, J.W. Cho, Y.K. Kwon, K.S. Ryu, I.K. Yu, S.Y. Hahn, Cryogenics 42 (2002) 351–355.

[6] T. Sels, C. Dragu, T.Van. Craenenbroeck, R. Belmans, New energy storage devices for an improved load managing on distribution level, in: IEEE Porto Power Tech Conference Proceedings, vol. 4, 2001, pp. 1–6.

[7] A. Abu-Siada, W.W.I. Keerthipala, W.B. Lawrance, Application of a superconducting magnetic energy storage unit to improve the stability performance of power systems, in: IEEE Canadian Conference on Electrical and Computer Engineering, 2002.

[8] M.D. Mufti, R. Balasubramanian, S.C. Tripathy, S.A. Lone, Int. J. Power Energy Syst. 23 (1) (2003) 24–36.

[9] G.S. Stavrakakis, G.N. Kariniotakis, IEEE Trans. Energy Convers. 10 (1995) 577–590.

[10] F. Zhou, G. Joos, C. Abbey, L. Jia, B.T. Ooi, Use of large capacity SMES to improve the power quality and stability of wind farms, in: Power Engineering Society General Meeting, IEEE 6–10 June, vol. 2, 2004, pp. 2025–2030.